Analysis of bias induced by various forward projection models in iterative reconstruction

K. Schmitt, H. Schöndube, K. Stierstorfer, J. Hornegger, F. Noo

***Abstract*—Discrete representation of the CT image is a major step in the design of iterative reconstruction algorithms, particularly because the decision being made at this level affects both bias and noise properties of the reconstruction, in addition to choices made later in the algorithm design. In this work, we examine the bias induced by popular image representation models, namely Joseph's method and the basis function approach relying on B-splines and blobs. Our preliminary results highlight a common weakness in terms of overshoot and undershoot artifacts at sharp boundaries. They also show that the Blobs may perform only as well as the B-spline of order two in terms of bias, and that Joseph's method tends to produce results that are fairly comparable to the B-spline of order one, with a slight advantage in favor of the latter.**

I. Introduction

Discrete representation of the CT image is a major step in the design of iterative reconstruction algorithms. Two commonly used techniques to represent the image with a finite number of unknowns are the sampling approach and the basis function approach. In the sampling approach, the image is represented by its values at a fixed number of locations that are typically equidistantly distributed in the direction of Cartesian coordinates. In the basis function approach, the image is represented by a finite linear combination of specific functions that are often selected as scaled and translated versions of a single function, called the mother function. Popular mother functions include the blobs [1] and the B-splines [2].

Since the basis function approach yields a continous model for the image, the definition of line integrals modelizing the CT measurements is straightforward when using this approach. For the sampling approach, the situation is different: defining line integrals with this approach requires the introduction of a numerical scheme. One widely-used scheme was suggested by Joseph [3]. Another more recent scheme that is gaining interest is the distance-driven technique suggested by De Man and Basu [4]. Note that both schemes process line integrals differently according to their slope, with the caveat that the involved approximation is usually less accurate for lines that are at 45 degrees relative to the Cartesian grid of samples used to represent the image.

Naturally, the performance of iterative reconstruction methods is affected by the choices made to represent the CT image and to model the CT measurements from this representation. Both bias and noise properties of the CT reconstruction can change dramatically according to these choices, as illustrated, for example, in [5], for the selection of parameters defining the blobs. In this work, we are interested in evaluating the bias induced by such choices. We will compare results obtained using blobs and B-splines together with results obtained using Joseph's method. The study is limited to two-dimensional CT imaging. In section II, we give a brief review on B-splines ans blobs. In section III, we present our experimental setting. Last, in section IV, we present and discuss preliminary results.

K. Schmitt, H. Schöndube and K. Stierstorfer are with Siemens AG, Healthcare Sector. J. Hornegger is with the Pattern Recognition Lab, University of Erlangen-Nürnberg, Erlangen, Germany. F. Noo is with the Department of Radiology, University of Utah, Salt Lake City, Utah, USA.

The concepts presented in this paper are based on research and are not commercially available. This work was partially supported by NIH grant R01 EB007236; its content is solely the responsibility of the authors and do not necesarily represent the official views of the NIH.

II. Image representation using basis functions

Here, we briefly review the basis function approach. Throughout this section and the rest of this abstract, we use $f(x,y)$ to denote the function that describes the linear attenuation coefficient of X-rays as a function of the position within the field-of-view of the scanner.

A. General concept

In the basis function approach, $f(x,y)$ is approximated by a linear combination of basis functions denoted as $f_a(x,y)$. When the basis functions are defined from a mother function, $b(x,y)$, the expression for $f_a(x,y)$ is as follows:

$$f_a(x,y) = \sum_{k,l} c_{kl} \cdot b((x-x_k)/\Delta x, (y-y_l)/\Delta y) \quad (1)$$

where the c_{kl} are the basis function coefficients to be estimated. In this expression, the locations $x_k = k\,\Delta x$ and $y_l = l\,\Delta y$ are samples on a Cartesian grid of size $N_x \times N_y$ with steps Δx and Δy in x and y, respectively. Often, Δx and Δy are selected to be equal. We make this assumption here and let $h = \Delta x = \Delta y$.

B. Line integrals

When using the basis function approach to represent $f(x,y)$, the Radon transform of f, denoted as $r(\theta,s)$, is simply approximated by the Radon transform of $f_a(x,y)$, denoted as $r_a(\theta,s)$. The linearity of the Radon transfrom yields

$$r_a(\theta,s) = \sum_{k,l} c_{kl} \cdot g(\theta, (s - x_k\cos\theta - y_l\sin\theta)/h) \quad (2)$$

where $g(\theta,s)$ is the Radon transform of $b(x,y)$.

C. B-splines

The B-splines are simple piecewise polynomial functions. They are defined by a single parameter: the degree, n, of the polynomial. The centered B-spline β_h^n of degree n and of width h is the $(n+1)$-th convolution of the normalized box function, β_h^0, with itself, i.e.,

$$\beta_h^n(x) = \beta_h^0 * \beta_h^{n-1}(x) = \underbrace{\beta_h^0 * \cdots * \beta_h^0}_{n+1\text{factors}} \tag{3}$$

with

$$\beta_h^0(x) = \begin{cases} 1/h, & \text{if } -h/2 \le x \le h/2 \\ 0, & \text{otherwise} \end{cases} \tag{4}$$

Using B-splines in the basis function approach means that $b(x,y) = \beta_h^n(x)\,\beta_h^n(y)$ is chosen. Let the one-sided power function be defined by

$$x_+^m = \begin{cases} x^m, & x \ge 0 \text{ and } m > 0 \\ 1, & x \ge 0 \text{ and } m = 0 \\ 0, & \text{otherwise} \end{cases} \tag{5}$$

Using this definition, it was shown in [2] that the Radon transform of $b(x,y)$ is

$$g(\theta,s) = \sum_{i=0}^{n+1}\sum_{j=0}^{n+1}(-1)^{i+j}\binom{n+1}{i}\binom{n+1}{j} \cdot \frac{\left[s + (\frac{n+1}{2} - i)\cdot h_1(\theta) + (\frac{n+1}{2} - j)\cdot h_2(\theta)\right]_+^{2n+1}}{(2n+1)!\,(h_1(\theta)\,h_2(\theta))^{n+1}} \tag{6}$$

where $h_1(\theta) = h\,|\cos\theta|$ and $h_2(\theta) = h\,|\sin\theta|$. Note that using the B-spline of order $n = 0$ for image representation is equivalent to adopting the approach of Siddon [6].

D. Blobs

The blob function is given by the following one-dimensional expression

$$\gamma_{m,a,\alpha}(r) = \begin{cases} \left(1 - \frac{r^2}{a^2}\right)^{\frac{m}{2}} \frac{I_m\left(\alpha\sqrt{1-\frac{r^2}{a^2}}\right)}{I_m(\alpha)} & \text{if } 0 \le r \le a \\ 0 & \text{otherwise} \end{cases} \tag{7}$$

where r is the radial distance from the blob center, a is the radius of the basis function, α is a parameter controlling the blob shape, and I_m is the modified Bessel function of order m.

Using blobs in the basis function approach means that $b(x,y)$ is chosen as $\gamma_{m,a,\alpha}(r)$ with $r = \sqrt{x^2+y^2}$. Given this definition, $g(\theta,s)$ is independent of θ, zero for $|s| > a$, and expressed as

$$g(\theta,s) = \left(\frac{2a^2\pi}{\alpha}\right)^{\frac{1}{2}} \left(1 - \frac{s^2}{a^2}\right)^{\frac{m}{2}+\frac{1}{4}} \frac{I_{m+\frac{1}{2}}\left[\alpha\left(1-\frac{s^2}{a^2}\right)^{\frac{1}{2}}\right]}{I_m\left[\alpha\right]}. \tag{8}$$

for $|s| < a$. Following the recommendations in [5], we chose $m = 2$, $a = 2$ and $\alpha = 10.4$.

III. Experimental setting

In this section, we describe the setting used for evaluation of the reconstruction bias and thereby compare the accuracy of various image representation models.

A. Phantom and data geometry

The FORBILD head phantom was used for all our evaluations. Also, a parallel-beam data acquisition geometry was assumed. Each CT measurement was simulated as an average of five line integrals that were calculated each using analytical expressions. The average was introduced to model the finite detector response (disregarding non-linearity effects) and reduce thereby high-frequency errors in the reconstruction process. The parameters defining our simulations are given in Table I.

B. Iterative reconstruction technique

Evaluating the bias in iterative reconstruction is not straightforward when the algorithm is non-linear. To circumvent this difficulty, we adopted a statistical model with no prior term. More specifically, the CT measurements were modelled as independent Gaussian deviates, and we seeked the maximum likelihood solution of minimum norm. Also, we assumed that the noise was stationary, which is a reasonable assumption for brain imaging with tube current modulation and beam-shaping bowtie filter.

Let c be the vector of unknown image coefficients, let g be the vector grouping the CT measurements, and let A be the matrix that links c to the CT measurements. Using this notation, the desired reconstruction can be expressed as the minimum-norm minimizer of $\|Ac - g\|$. This reconstruction was seeked using the Landweber algorithm, i.e., using the following iterative procedure:

$$c^{(k+1)} = c^{(k)} + \lambda\, A^T(g - Ac^{(k)}) \;, \tag{9}$$

where the convergence-controlling factor, λ, was chosen as 0.95 times $2/\sigma_{max}^2$, where σ_{max} is the maximum singular value of the projection matrix A. Thus, convergence was guaranteed and nearly as fast as possible. The quantity σ_{max} was computed using five iterations of the power method.

As it is well-known, resolution improves with the number of iterations, but discretization errors also increase at the same time, so that the maximum-likelihood reconstruction is not satisfactory. Hence, we focused on examining regularized reconstructions obtained by stopping the iterative process after a fixed number m of iterations.

C. Bias evaluation

Bias was evaluated using visual inspection of images and profiles, and also by calculing the reconstruction error over pixels located within the large central low-contrast ellipse within the phantom. The error was computed as the absolute difference between the reconstructed value and the true attenuation value for this ellipse, which is 1.045 ($45\ HU$).

D. Resolution measurement

As discussed earlier, resolution in the reconstruction typically improves with the number of iterations. To evaluate resolution, we opted for the modulation transfer function (MTF). Computation of this function was performed with the following steps: (i) a phantom that consists only of the

	image discretization	CT measurement
matrix size	350×350	700×380
	$(N_y \times N_x)$	(views $\times$ rays-per-view)
sampling step	$\Delta x = \Delta y = 0.075$	$\Delta s = 0.075$

TABLE I
IMAGE REPRESENTATION AND CT MEASUREMENT PARAMETERS.

low-contrast ellipse within the FORBILD head phantom was defined, (ii) CT measurements for this ellipse were generated in the same way as measurements for the full phantom, (iii) reconstruction was performed from these measurements, (iv) an edge profile that gives the reconstructed value as a function of the distance from the ellipse was computed from the reconstruction, (v) the MTF was obtained as the Fourier transform of the edge profile.

Given the linearity of the chosen reconstruction method, the methodology above was suitable for assessment of the resolution achieved within the neighborhood of the large low-contrast ellipse in reconstructions of the FORBILD head phantom.

IV. PRELIMINARY RESULTS AND DISCUSSION

First, we examined the reconstructions obtained using both a small and a large number of iterations, which were chosen as 250 and 850. Figure 1 shows the reconstruction results obtained using 250 iterations, and Figure 2 shows a vertical profile through these results, which passes through the left eye. Figures 3 and 4 shows the reconstruction results and profiles for 850 iterations. These figures highlight significant differences between the different image representations. They also show that, irrespective of the selected representation, increasing the number of iterations amplifies the magnitude of overshoots and undershoots errors at the sharp boundaries while reducing their spread; note that these errors are present despite the low-pass filtering that was applied in the data simulation process.

Figure 5 shows the MTF curves corresponding to each image representation for both 250 and 850 iterations. From these plots, it can be seen that, not unexpectedly, resolution varies from one representation to the other and also changes at a different pace for each representation. For a fair comparison, it is needed to take these differences into account. An attempt at such a comparison is shown in Figure 6, where the bias metric discussed in section III.C is displayed as a function of the mean MTF value.

Under the assumption that the mean MTF value is acceptable as a summary measure for resolution, the following observations can be made from Figure 6, some of which were already well-known:

- The B-spline with $n = 0$ produces the largest bias.
- Joseph's method performs almost as well as the B-spline of order $n = 1$, with a slight difference in favor of the B-spline that is most likely due to Joseph's method yielding a reduced accuracy along lines that are at 45 degrees.
- The B-spline of order $n = 2$ performs as well as the blobs.

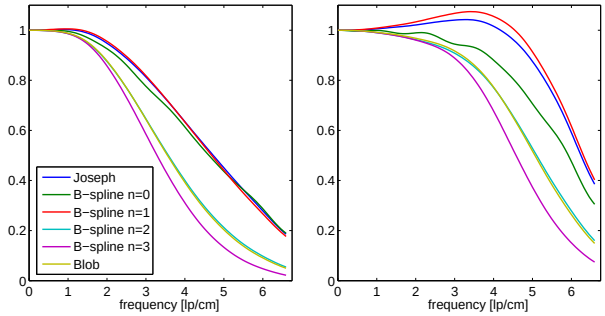

Fig. 5. *left:* Modulation transfer function (MTF) for reconstructions based on 250 and 850 iterations of the Landweber algorithm, using the basis function approach with the blobs and the B-splines, and also using Joseph's method.

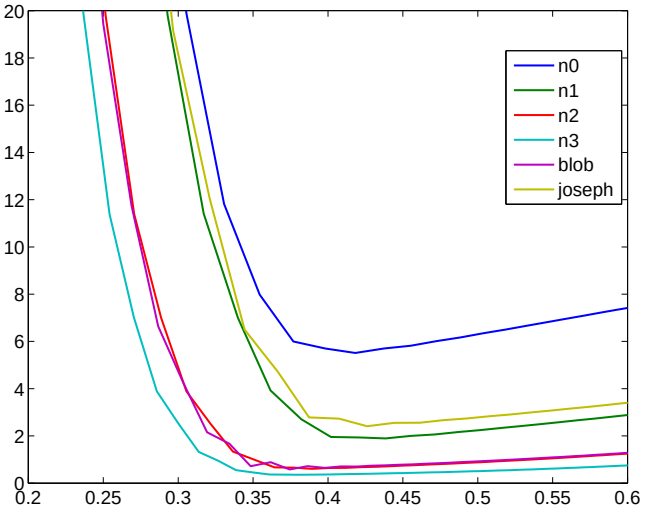

Fig. 6. *left:* Bias-versus-resolution curves obtained by varying the number of iterations by steps of 5. The bias is expressed in HU.

- The B-spline of order $n = 3$ outperforms the blobs.

In future work, we will examine closer the impact of the summary measure being chosen for the MTF curve, and we will also extend our study to include the distance-driven technique [4].

REFERENCES

[1] R. M. Lewitt, *Multidimensional digital image representations using generalized Kaiser-Bessel window functions*, J. Opt. Soc. am. a, 7(10), pp. 1834-46, 1990.

[2] S. Horbelt et al., *Discretization of the Radon Transform and of its Inverse by Spline Convolutions*, IEEE Transactions on Medical Imaging, 21(4), pp. 363-76, 2002.

[3] P. M. Joseph, *An Improved Algorithm for Reprojecting Rays Trough Pixel Images*, IEEE Transactions on Medical Imaging, 1(3), pp. 192-96, 1982.

[4] B. De Man, S. Basu, *Distance-driven projection and backprojection in three dimensions*, Physics in Medicine and Biology, 49, pp. 2463-75, 2004.

[5] S. Matej and R. M. Lewitt, *Practical considerations for 3-D image reconstruction using spherically symetric volume elements*, IEEE Transactions on Medical Imaging, 15(1), pp. 68-8, 1996.

[6] R. L. Siddon, *Fast calculation of the exact radiological path for a three-dimensional CT array*, Med. Phys., 12(2), pp. 252-55, 1985.

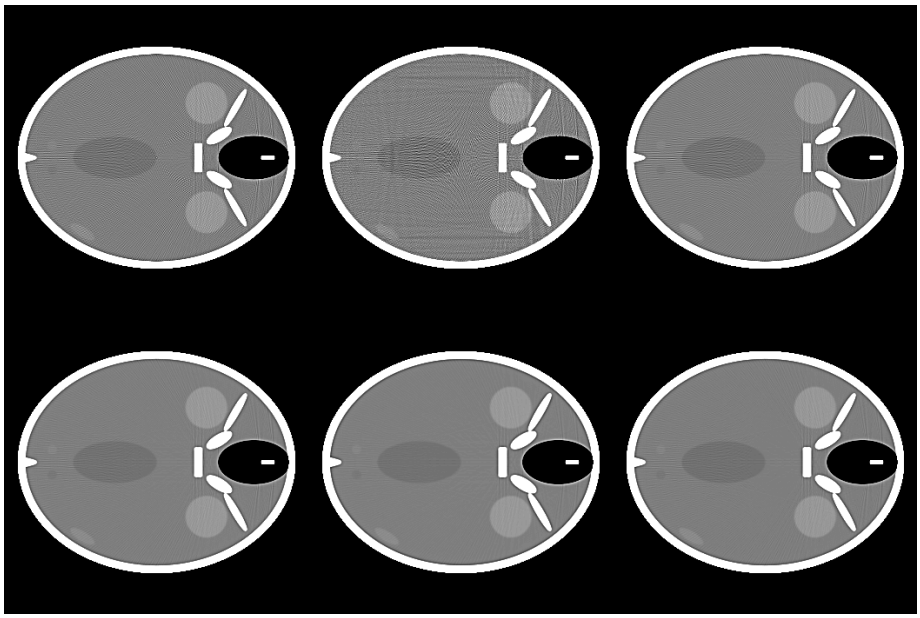

Fig. 1. Reconstruction using 250 iterations of the Landweber algorithm, using Joseph's method (top row, left image); using the B-splines of order $n = 0$ (top row, middle image), $n = 1$ (top row, right image), $n = 2$ (bottom rowm, left image) and $n = 3$ (bottom row, middle image); and using the blobs (bottom row, right image). Grayscale: [1,1.1].

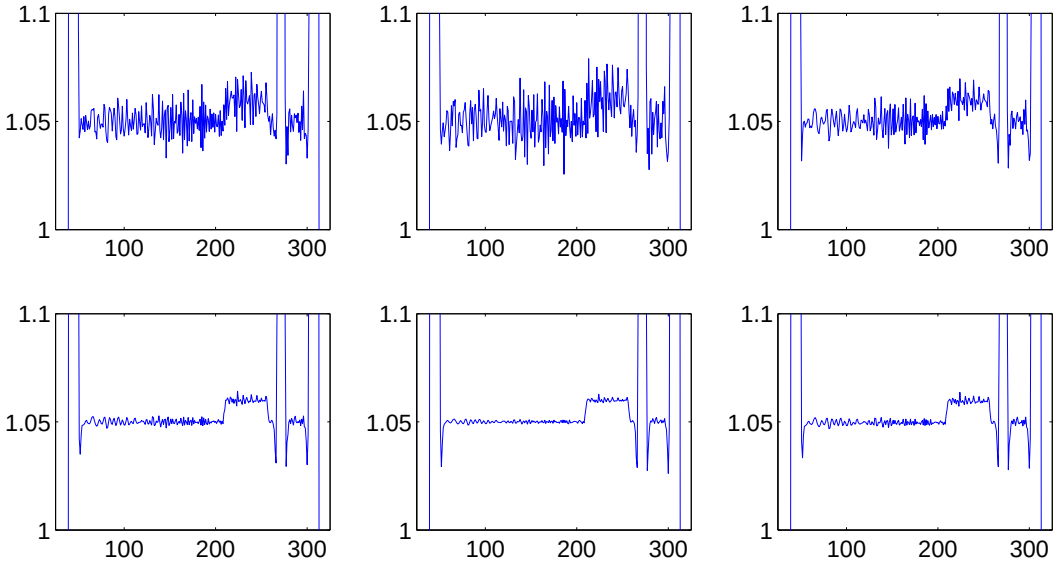

Fig. 2. Profile through the left eye for the reconstructions based on 250 iterations. Same arrangement is as in Fig. 1.

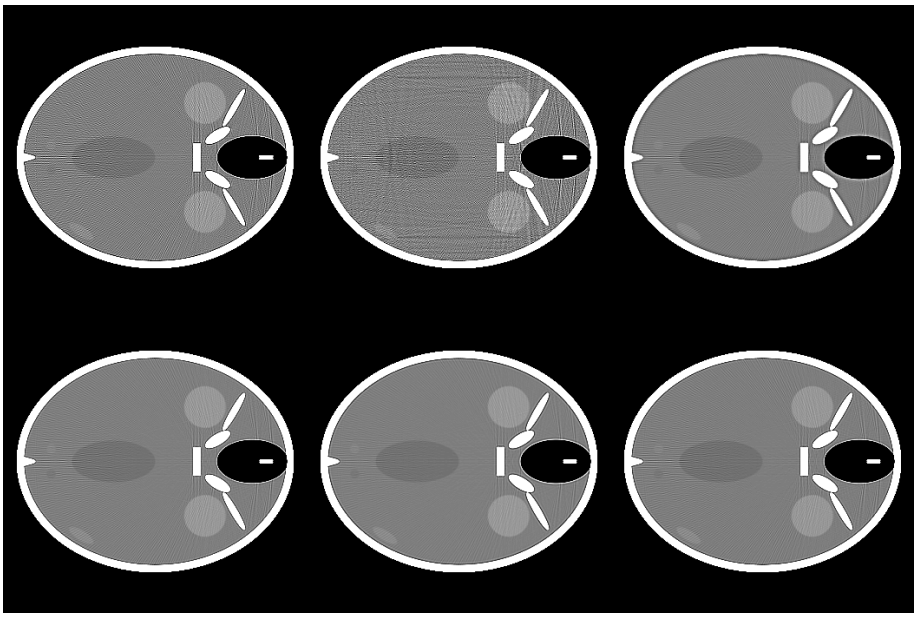

Fig. 3. Iterative reconstruction using 850 iterations of the Landweber algorithm. Grayscale: [1,1.1]. Same arrangement is as in Fig. 1.

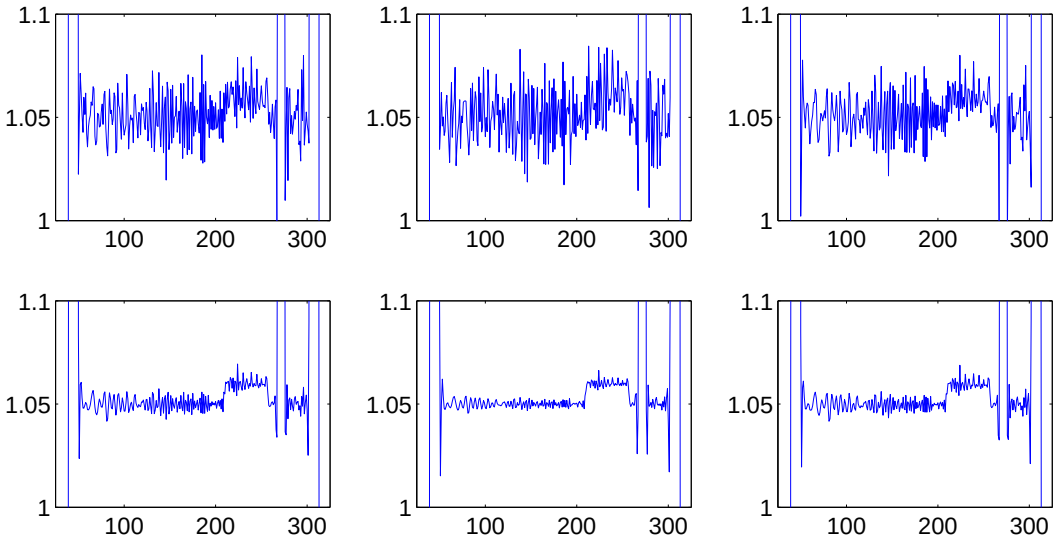

Fig. 4. Profile through the left eye for the reconstructions based on 850 iterations. Same arrangement is as in Fig. 1.